Low resolution structural studies of apoferritin via SANS and SAXS: the effect of concentration

T. N. MURUGOVA[a,b], A. V. VLASOV[b], O. I. IVANKOV[a,c], A. V. ROGACHEV[a,b], YU. L. RYZHYKAU[b], D. V. SOLOVIOV[a,c], A. ZHIGUNOV[d], E. V. ZINOVEV[b], YU. S. KOVALEV[a,b], A. ROUND[f], V. I. GORDELIY[a,b,e,g], A. I. KUKLIN[a,b*]

[a]*Joint Institute for Nuclear Research, Dubna, Russia*
[b]*Moscow Institute of Physics and Technology, Dolgoprudniy, Russia*
[c]*Taras Shevchenko National University of Kyiv, Kyiv, Ukraine*
[d]*Institute of Macromolecular Chemistry CAS, Prague, Czech Republic*
[e]*Institute of Complex Systems (ICS), ICS-5: Molecular Biophysics, Research Centre Juelich, 52425, Juelich, Germany*
[f]*EMBL, 6 Jules Horowitz, F-38042 Grenoble, France*
[g]*Institute of Structural Biology J.P.Ebel, Grenoble, France*

The results of small angle scattering investigation of protein apoferritin are presented. In particular, the results of approximation to zero value of concentration are calculated. The procedure of approximating at zero concentration of apoferritin in this work is considered. The sizes and shapes, including those determined by indirect Fourier transform method, obtained on different instruments are compared. The pair-distance distribution function for both small angle neutron (SANS) and X-ray scattering (SAXS) is computed. It is shown that SANS and SAXS methods give similar form factor (spherical shell with holes) of apoferritin. At the same time, fits of experimental data for SAXS and SANS curves give different sizes and volumes of the molecule. The reasons for these discrepancies are discussed.

(Received August 17, 2015; accepted September 9, 2015)

Keywords: Small-angle X-ray and neutron scattering, Apoferritin, Concentration effect, Instrument comparison

1. Introduction

Small-angle scattering (SAS) is the one of the soft matter investigation methods. This method could be used for polymers, for biological and material science objects as well as exotic bubbles in water [1] or fractal organization of soil [2]. But SAS technique has a range of limitations and in comparison with electron microscopy can bring to different results for the same scattering picture. One more problem is a form and size polydispersity of the particles [3,4]. In case of monodisperse samples (for example, dendrimers [5-8] or track membranes [9,10] the major integral parameters and *a priori* knowledge about the shape of the molecules should give only one solution [11].

In this work we investigated a protein ferritin, which plays a key role in iron metabolism. The name of "ferritin" was given by V. Laufberger due to protein contained over 20% (wt/wt) iron according to [12, 13].

Ferritin is a protein which resolves the oxide radicals and iron storage problems. The technical applications of ferritin with modified central part are also discussed. As it is well known, ferritin is a large protein, consists of 24 ferritin polypeptides and comprises central part containing iron based molecules. The apoferritin is a protein complex which is a ferritin shell (without iron core).

Apoferritin with mineral nucleus forms the ferritin – apoferritin protein or its analogues have been found in all living organisms [14-16].

First investigation of iron metabolism were started in 1940-th by Granick [17], magnetic properties of ferritin and ferric compounds [14] and the mechanisms of iron metabolism were also proposed [19-21]. First X-ray diffraction experiments with the ferritin were performed in the 40-th of previous century [22]. Nevertheless, at present, there is still quite big activity in the field. Recently, the structure of protein-protein complexes in physiological solution has received much attention [23]. Despite the fact that a lot of structures of these complexes are presented in PDB bank and the history of their studies is quite long there are still several open questions. In particular, recent structural studies are focused on interparticle correlations [24], and the protein complex appeared to be very useful as a test sample for SAS instruments [25].

The aim of this work is to continue applying recent SAS approaches to low resolution studies of the protein complexes mentioned above with a particular goal – to compare SAXS and SANS structures obtained in such way [26].

2. Materials and methods

Horse spleen apoferritin was purchased from Sigma-Aldrich Chemie GmbH (Product number A3660). Storage buffer (50% glycerol and 0.075 M NaCl) was replaced for buffer contained 150 mM NaCl and 5 mM Na_2HPO_4,

pH=7.3. The buffer for neutron experiment was based on heavy water granting best contrast and decreasing incoherent background. The buffer for X-ray experiments was based on H_2O. The buffer replacement was fulfilled by centrifugal ultrafiltration with filters Centricon Y-100 (Millipore corporation). The final concentration of protein was 25 mg/ml for SANS experiments and 50 mg/ml for SAXS.

The neutron experiments were performed at YuMO spectrometer with two detectors system mode [27, 28]. The beam was collimated to a diameter of 14 mm on the sample. The obtained spectra were put on absolute intensity scale using vanadium scatterer. Spectra were normalized by the standard procedure using SAS software [29]. The investigations by small angle X-ray (SAXS) method were carried out on Rigaku instrument which is available at the Moscow Institute of Physics and Technology (Dolgoprudny, Russia) [30] and bioSAXS beamline BM29, ESRF, Grenoble, France [31].

Rigaku SAXS instrument has a pinhole camera attached to a rotating anode X-ray high-flux beam generator (MicroMax 007-HF) which operates at 40 kV and 30 mA (1200 W). The camera was equipped with a multiwire, gas-filled area detector with an active area diameter of 20 cm. Two experimental chambers were used to cover the Q-range of 0.006 – 1.4 Å ($Q = \frac{4 \cdot \pi}{\lambda} \cdot \sin\Theta$, where λ is the wavelength and 2θ is the scattering angle).

The working energies of BM29 were between 7 to 15 keV. Despite this is a bending magnet beamline, an elevated flux at detector plane was achieved thanks to the double multilayer monochromator (energy band pass ~ 10^{-2}) and 4 mrad torodial mirror 1.1 m long. Experimental hutch is equipped with a marble table housing the modular-length flight tube, 2D detector (Pilatus 1M) and a sample handing equipment (automated sample changer). The achievable Q-range is 0.025 - 5 nm^{-1}, which corresponds to the biggest measurable R_g (radius of gyration) of the investigated particle of 20 nm. Data collection, processing and analysis were performed in an automated manner using dedicated beamline software BsxCuBE [32].

3. Results and discussion

3.1 Concentration effect

To calculate the parameters accurately it is necessary to take in account the influence of the concentration on the SAS curves. For this purpose we have chosen samples with low concentrations and made an approximation at zero concentration. [Fig.1] represents a set of raw data obtained on the bioSAXS beamline BM29, ESRF, Grenoble, SAXS.

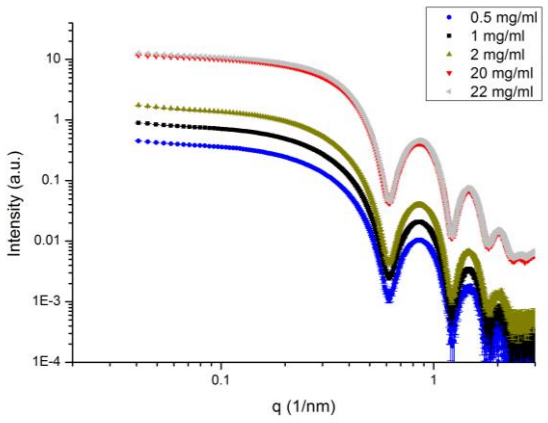

Fig.1. SAXS curves for apoferritin water solution. Each curve corresponds to different concentration. Concentrations from the top to the bottom are: 22, 20, 2, 1, 0.5 mg/ml.

The data treatment was made by Zimm method [33]. We calculated the curve at zero value of concentration from the formula of the SAS intensity:

$$I(Q) = c \cdot |F(Q)|^2 \cdot S(Q) \qquad (1)$$

where $|F(Q)|^2$ – the account of the form-factor, $S(Q)$ – structure factor, $S(Q) \to 1$ with $c \to 0$ and thus (1) gives:

$$\left(\frac{I}{c}\right)_{c \to 0} = |F(Q)|^2 \qquad (2)$$

And here one can see that obtained curve corresponds to the form-factor of apoferritin only.

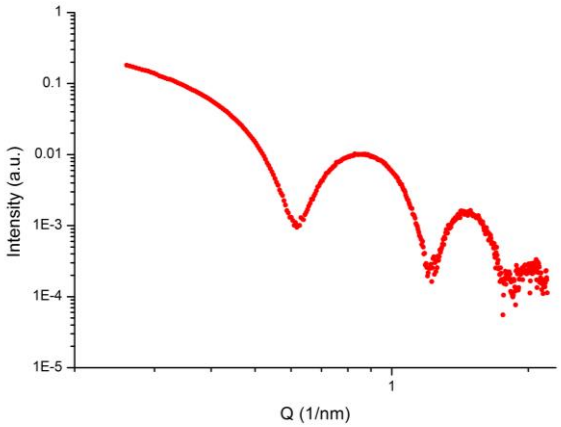

Fig. 2. Intensity divided concentration as results of approximation to zero concentration for apoferritin (see eq.(5)).

Here, we should notice that only low concentrations of apoferritin were used for data analysis by Zimm method, namely 0.97 mg/ml, 1.93 mg/ml, 3.96 mg/ml and 4.97 mg/ml. For linear fit we used only these concentrations. Higher concentrations such as 38.0 mg/ml and 40.8 mg/ml cannot be used for linear fit in Zimm method.

Also from the [Fig. 2] one can see that at $Q > 1$ (1/nm) the significant errors take place. To avoid errors we substituted part of the curve, containing errors, for one corresponding to the highest concentration of the protein because there is no influence of the structure factor in $Q > 1$ (1/nm). So, we built a curve corresponding to zero concentration in maximum Q-range [Fig. 3].

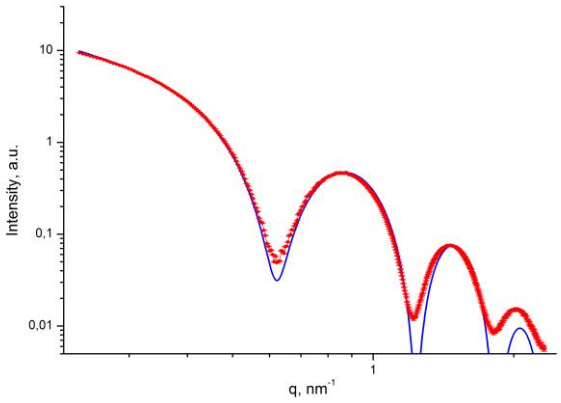

Fig. 3. SAXS curve obtained by Zimm method for apoferritin (see eq. (5)) in maximum Q-range (solid circles) and its fitting by program SASfit using spherical shell model (line).

3.2 Monodisperse and polydisperse systems

The difference in SAS curves occurs when one has to deal with polydisperse systems. For example, the aqueous solution of apoferritin has a tendency of clustering even at low concentrations (< 1mg/ml) and the investigation of the SAS curves behaviour for dimeric and trimeric apoferritin molecules show the significant difference in small-angle Q-region in a comparison with the monomeric molecules solution. But this question is out of the scope of the paper.

3.3 The pair-distance distribution function

The pair-distance distribution function P(r) was obtained using indirect Fourier transformation of experimental small angle neutron scattering data treatments for apoferritin. The function P(r) was reconstructed using program GNOM [34] of ATSAS program package [35]. The pair-distance distribution function (P(r)) obtained by this procedure and its approximation of experimental curves are shown in [Fig.4]. Functions are bell-shaped, the maxima of this function are shifted from the center position, which indicates the displacement of the scattering density from the center (unlike for spherical shell) to the periphery of the molecule. The maximum of the P(r) function corresponds to the most probable distance between two points in a protein molecule. This distance is about 85 Å. For the received pair-distance distribution functions P (r) the values of the radii of gyration, according to the [36], are 51.3Å and 51.7Å (52.4Å) according to the SANS and SAXS, respectively. The values of the radius of gyration obtained from the indirect transform are equal to those obtained previously from fitting the experimental curves by the model of spherical shell scattering function. From the indirect transform, we can also estimate the maximum size of protein molecule, which is about 120 Å.

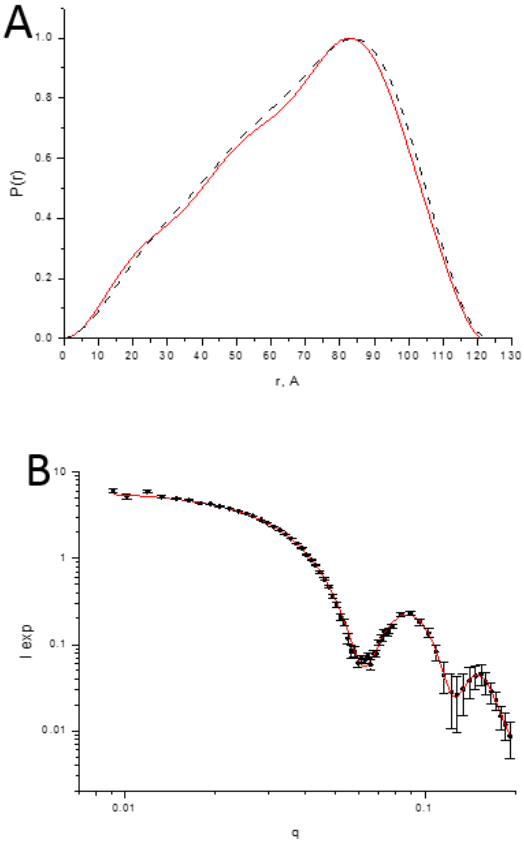

Fig.4 The result of the pair-distance distribution function reconstruction for the apoferritin molecule for small-angle neutron scattering (SANS) and X-ray (SAXS). (A) Pair-distance distribution function P(r) SANS (continuous line) and X-ray (SAXS) (dash line). (B) Fit of SAXS experimental data by the scattering curve calculated from P(r).

3.4 Three-dimensional model

Three-dimensional model of apoferritin molecule built by Monte-Carlo method is shown on the [Fig.5].

Often, three-dimensional representation of the object's shape can be obtained by fitting the experimental scattering curve by theoretical one, which corresponds to the selected model. Having no *a priori* information about the object structure could be done the model is built by an algorithm, implemented in the program DAMMIF using small-angle scattering data [37]. This algorithm uses the

Monte Carlo method and represents a model of an object as a set of small spheres (dummy-atoms). The resulting model is a low resolution one, because SANS method is a representative of low-resolution techniques, which give structural information in the range 10-1000 Å. The scattering intensity for the dummy-model is calculated as follows:

$$I(Q) = 2 \cdot \pi \cdot 2 \cdot \sum_{l=0}^{\infty} \sum_{m=-l}^{l} \left| A_{lm}(Q) \right|^2 \qquad (3)$$

where A_{lm} amplitude is calculated as:

$$A_{lm}(Q) = i^l \cdot \sqrt{\frac{2}{\pi}} \cdot \nu_a \cdot \sum_{\substack{j=1 \\ X(j)=1}}^{M} j_l(Q \cdot r_j) \cdot Y^*_{lm}(\omega_j) \qquad (4)$$

(r_j, ω_j) – spherical coordinates,

$\nu_a = \frac{4\pi r_0^3}{3} \frac{1}{0.74}$ – dummy-atom volume, $Y^*_{lm}(\omega_j)$ – corresponding spherical harmonic, $j_l(\mathrm{Q} r_j)$ – Bessel function. For the optimal fitting the following function f (X) should be minimized:

$$f(X) = R^2(I, X) + \sum_k \alpha_k P_k(X), \qquad (5)$$

The first term is the model intensity deviation from the experiment, the second term is the sum of penalties imposed on the solution, with their weights. The simulation result is a compact model of the balls that approximates the experimental data of small-angle scattering in the best way according to (4).

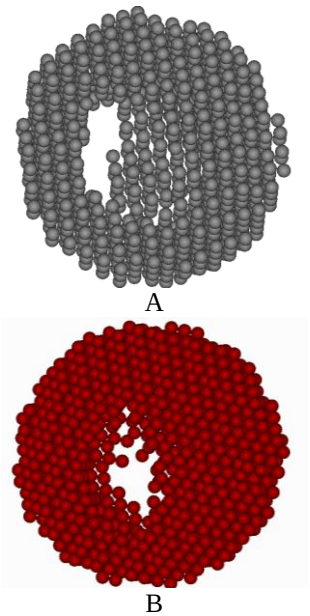

A

B

Fig.5 The projection of apoferritin 3D model obtained by DAMMIF program for SANS (A) and for SAXS (B).

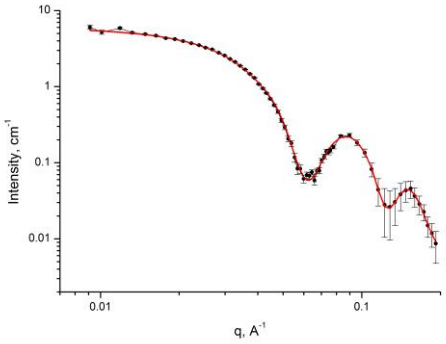

C

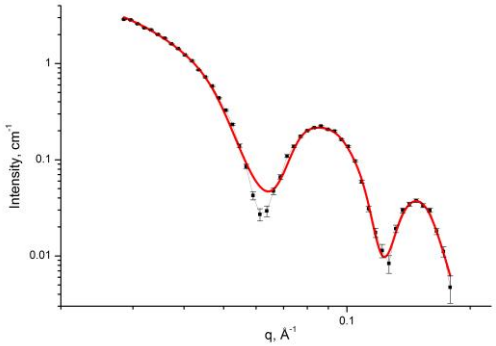

D

Fig.6 Approximations (solid lines) of experimental curves (squares) for each 3D model for SANS(C) and SAXS (D) correspondently.

SANS and SAXS data for the apoferritin solution were treated by the DAMMIF program. The projections of the obtained structures are shown in [Fig.4]. The model is a spherical shell with outer and inner diameters of about 120 Å and 75 Å respectively. The volume of this structure is 510x10^{3}Å^3 for SANS and 640x10^{3}Å^3 for SAXS. There are "holes" in the shell, which could appear due to the problem of instability solution due to the small thickness of the protein shell (20 Å) due to specifics of algorithm or by the presence of regions in the protein shell with the same scattering density as for the solvent. Last assumption requires further analysis.

1.1. The scattering curves approximation by spherical shell function

According to the crystallographic data (Protein Data Bank, PDB) and data obtained by authors using DAMMIF program, the apoferritin molecule could be defined by a spherical shell. The neutron and x-ray scattering curves for apoferritin were approximated by the scattering function for a spherical shell (6):

$$I_{sph}(\mathrm{Q}) = \left[V_1 \Phi(\mathrm{Q} R_1) - V_2 \Phi(\mathrm{Q} R_2) \right]^2, \qquad (6)$$

where

$$V_1 = \frac{4}{3} \pi R_1^3,$$

$$V_2 = \frac{4}{3}\pi R_2^{\,3},$$

$$\Phi(t) = 3\frac{\sin t - t\cos t}{t^3},$$

R_1 and R_2 – outer and inner spherical shell radius correspondingly.

For a spherical shell the radius of gyration, inner and outer radii are related as:

$$R_g = \sqrt{\frac{3}{5}\frac{R_1^{\,5} - R_2^{\,5}}{R_1^{\,3} - R_2^{\,3}}} \qquad (7)$$

Experimental curves approximations were carried out by programs Fitter 2.1.2 [38], SasView 3.0.0 [39] and SASfit 0.94.6 [40] (presented in [Fig. 3]). The maximum size of molecule is $2R_1$ and the volume of the spherical shell is:

$$V_{shell} = \frac{4}{3}\pi(R_1^{\,3} - R_2^{\,3}) \qquad (8)$$

Table 1. Main parameters were calculated from experimental scattering curves were obtained by SANS and SAXS instruments.

№	Parameter	SANS (YuMO)	SAXS (Rigaku)	SAXS (BM29)
1	Outer radius, R_1, Å	59.1 ± 0.3	62.0 ± 0.1	62.5 ± 0.5
2	Inner radius R_2, Å	40.1 ± 0.4	37.5 ± 0.1	37.1 ± 0.5
3	Radius of Gyration R_g,Å	51.1 ± 0.3	52.2 ± 0.1	52.4 ± 0.2
4	Radius of Gyration (from P(r)), R_g,Å	51.3	51.7	52.4
5	Volume of Shell, Vp, $x10^3$ Å^3	590 ± 20	780 ± 20	807 ± 15
6	Volume Vp $x10^3$ Å^3	560* 510**	680* 640**	785*

* - *volumes calculated from Porod approximation;*
** - *volumes obtained by DAMMIF program.*

Radius of gyration and volume were calculated from pair-distance distribution functions P(r) and Porod approximation respectively. In addition, we show the volume values obtained by DAMMIF program of ATSAS program package [35]. Also this values were calculated according to Eqs.(7,8). R1 and R2 values were calculated by programs Fitter [38], SasView [39] and SASfit [40]. The errors of parameters values in lines 1-3 and 5 [Table 1] were calculated from fitting procedure.

4. Conclusion

In this work we showed the results of small angle scattering investigation of protein apoferritin. Despite the fact that apoferritin in water solution is a monodisperse macromolecule, the influence of the structure factor is noticeable even at low concentrations. We calculated the SAS curve corresponding to zero concentration of apoferritin. For this purpose Zimm method was used. Then we substituted part of this curve for one corresponding to the highest concentration to avoid errors in high Q-range. As a result we got the SAS curve without structure factor contribution in maximum Q-range.

Obtained SANS and SAXS (BM29) data for the apoferritin in solution were treated by the DAMMIF program. The structural models correspond to spherical shell with outer and inner diameter of about 125 Å and 76 Å respectively. The shape and 3D model obtained by the low resolution method are consistent with the known results (PDB bank data). The calculated volumes for the models of the molecules is $590x10^3$Å^3 and $780x10^3$Å^3 ($807x10^3$Å^3) for SANS and SAXS data respectively, however, the apoferritin molecule volumes determined from Porod approximation are $560x10^3$Å^3 and $660x10^3$Å^3 ($785x10^3$Å^3) for SANS and SAXS, respectively. We have observed a slight systematic difference of structural parameters obtained for SAXS and SANS data. This can occur due to partially substitution of a protein shell hydrogen for deuterium. We suggest that this should be taken into account in the interpretation of the results of low resolution studies of proteins.

Acknowledgements

We greatly acknowledge support of this work by the Russian Foundation for Basic Research (project 13-02-01460_a). This work was supported by the Russian Foundation for Basic Research (research project 13-04-91320) and the Helmholtz Association of German Research Centers (project HRJRG-401).

We are grateful to Dr. V. Borshchevskiy and A. Mishin for fruitful discussion.

This work benefited from SasView software, originally developed by the DANSE project under NSF award DMR-0520547.

References

[1] N. F. Bunkin, O. I. Vinogradova, A. I. Kuklin, A. V. Lobeev, T. G. Movchan, JETP Letters **62**(8), 685 (1995).

[2] G. N. Fedotov, Y. D. Tret'yakov,V. K. Ivanov, A. I. Kuklin, E. I. Pakhomov, A. K. Islamov, T. N. Pochatkova, Doklady Chemistry **405,** 240 Part: 1 (2005).

[3] M. Balasoiu, I. Bica, Yu.L. Raikher, E.B. Dokukin, L. Almasy, B. Vatzulik, A.I. Kuklin. Optoelectron. Adv. Mater. – Rapid Comm. **5**(5), 523 (2011).

[4] M. Balasoiu, L.A. Ischenko, S.V. Stolyar, R.S. Iskhakov, Yu.L. Raikher, A.I. Kuklin, D. V. Soloviov, T. S. Kurkin, D. Aranghel, G. M. Arzumanian. Optoelectron. Adv. Mater. – Rapid Comm. **4**(12), 2136 (2010).
[5] Alexander I. Kuklin, Alexander N. Ozerin, Akhmed Kh.Islamov, Aziz M.Muzafarov, Valentin I.Gordeliy, Eugeniy A. Rebrov, Galina M. Ignat'eva, Elena A. Tatarinova, Ruslan I.Mukhamedzyanov, Lyudmila A.Ozerina Eugeniy Yu.Sharipov, J. Appl.Cryst. **36**, 679 (2003).
[6] A. N. Ozerin, A. M. Muzafarov, A. I. Kuklin, A. Kh. Islamov, V. I. Gordelyi, G. M. Ignat'eva, V. D. Myakushev, L. A. Ozerina, E. A. Tatarinova, Doklady Chemistry **395**(2), 59 (2004).
[7] Alexander N. Ozerin, Aziz M.Muzafarov, Valentin I. Gordeliy, Alexander I. Kuklin, Galina M. Ignat'eva, Mikhail A.Krykin, Lyudmila A.Ozerina, Natalia A. Shumilkina, Akhmed Kh.Islamov, Eugene Yu. Sharipov, Ruslan I. Mukhamedzyanov, Macromol. Symp. **195**, 171 (2003)
[8] A. N. Ozerin, D.I. Svergun, V.V. Volkov, A.I.Kuklin, V.I.Gordeliy, A.K.,Islamov, D.S.Zavorotnyuk, J.Appl.Cryst. **38**(6), 996 (2005).
[9] Gerard Pepy, Emmanuel Balanzat, Bruno Jean, Alexandr Kuklin, Nadejda Sertova and Marcel Toulemonde, J.Appl.Cryst. **36**, 649 (2003).
[10] Gerard Pepy, Peter Boesecke, Alexandr Kuklin, Emmanuel Manceau, Birgitta Schiedt, Zuzanna Siwy, Marcel Toulemonde and Christina Trautmann, J. Appl. Cryst. **40**, 388 (2007).
[11] A. V. Rogachev, A. Yu. Cherny, A. N. Ozerin, V. I. Gordeliy, and A. I. Kuklin. ISSN 1063-7745, Crystallography Reports. **52**(3), 500 (2007).
[12] N Kresge, R.D.Simoni and R.L.Hil, Journal of Biological Chemistry **279** e9-e11 (2004).
[13] V.Laufberger, Bulletin de la Société de chimie biologique **19,** 1575 (1937).
[14] S.C. Andrews Advances in Microbial Physiology, ed. R. K. Poole. Academic Press. 281-351 (1998).
[15] R.R.Crichton and R.J.Ward, Met Ions Biol Syst **35** 633 (1998).
[16] W.H.Massover, Micron **24** 389 (1993).
[17] S.Granick, Journal of Biological Chemistry **149** 157 (1943).
[18] L. Michaelis, C.D.Coryell and S.Granick, Journal of Biological Chemistry **148** 463-80 (1943).
[19] D.M. Lawson, P.J. Artymiuk, S.J.Yewdall, J.M.A. Smith, J.C. Livingstone, A.Treffry, A. Luzzago, S. Levi, P. Arosio, G. Cesareni, C.D. Thomas,W.V. Shaw and P.M. Harrison, Nature **349,** 541 (1991).
[20] W.H. Massover Iron Biominerals, ed F.B. Frankel R.P.Blakemore. New York: Plenum Press, pp 349-58 (1991).
[21] W.H. Massover, 50-th Annual Meeting Electron Microcs. Soc. Am., ed San Francisco: San Francisco Press (1992) pp.1012-31992.
[22] I. Fankuchen , J. Biol. Chem. **150,** 57 (1943).
[23] C. Pons, M.D'Abramo, D.I. Svergun, M. Orozco P. Bernadó, J. Fernández-Recio, J Mol Biol **403**(2), 217-30 (2010).
[24] W.Häußler, A.Wilk, J.Gapinski and A. Patkowski. The Journal of chemical physics **117**(1), 413 (2002).
[25] H.Toyokawa, T.Fujisawa, Y.Inoko, T.Nagayoshi, Y. Nishi, Y.Nishikawa, A.Ochi, M.Suzuki T.Tanimori. NIM A: Accelerators, Spectrometers, Detectors and Associated Equipment Part 2 1144-7, 467-468 (2001).
[26] A.I. Kuklin, T.N. Murugova, O. I. Ivankov, A. V.Rogachev, D.V.Soloviov, Yu.S.Kovalev, A.V. Ishchenko, A. Zhigunov, T. S.Kurkin, V.I. Gordeliy, Journal of Physics: Conference Series **351**. No. 1. IOP Publishing, (2012).
[27] A.I. Kuklin, A.Kh. Islamov, V.I. Gordeliy, Neutron News **16(3)**, 16 (2005).
[28] A.I. Kuklin, A.Kh. Islamov, Yu.S. Kovalev, P.K. Utrobin, V.I. Gordeliy, Journal of Surface Investigation: X-ray, Synchrotron and Neutron Techniques **6,** 74 (2006).
[29] A.G. Soloviev, T.M. Solovieva, A.V. Stadnik, A.Kh.Islamov and A.I.Kuklin, Communication of JINR P10-2003-86, Dubna, (2003).
[30] Alexey Vlasov, Tatiana Murugova, Sergey Grudinin, Oleksandr Ivankov, Dmytro Soloviov, Andrey Rogachev, Adam Round, Yury Ryzhykau, Alexey Mishin, Taras Balandin, Valentin Borschevskiy, Valentin Gordeliy, Alexander Kuklin, FEBS Journal **281**, Issue Supplement s1, p. 593 (2014).
[31] P. Pernot, A.Round, R.Barrett, A. De Maria Antolinos, A.Gobbo, E.Gordon,S. McSweeney, Journal of synchrotron radiation. **20**(4), 660 (2013).
[32]URL:http://www.esrf.eu/UsersAndScience/Experiments/MX/About_our_beamlines/BM29
[33] L.A.Feigin and Dimitrij I. Svergun. Ed. George W. Taylor. New York: Plenum Press, 1987.
[34]D. Svergun, J.Appl.Cryst. **25,** 495 (1992).
[35] Data analysis software ATSAS 2.3.
[36] D. Svergun, J.Appl.Cryst. **24,** 485 (1991).
[37] D. Franke and D.I. Svergun. J.Appl.Cryst. **42**, 342 (2009).
[38] A.G. Soloviev, T.N. Murugova, A. H. Islamov A.I.Kuklin, Journal of Physics: conference series **351,** 012027 (2012).
[39] URL: http://www.sasview.org
[40] URL:http://kur.web.psi.ch/sans1/SANSSoft/sasfit.html

*Corresponding author: kuklin@nf.jinr.ru